

Type of the Paper (Article)

Anomalous Ca-content dependence of dielectric property of charge ordered $\text{Pr}_{1-x}\text{Ca}_x\text{MnO}_3$ as a signature of charge-ordered phase modulation

Ankit Kumar Singh ¹ and Partha Sarathi Mondal ^{2*}

¹ Department of Applied Sciences and Humanities, National Institute of Advanced Manufacturing Technology, Ranchi 834003, India, ankit.cuj2408@gmail.com

² Department of Applied Sciences and Humanities, National Institute of Advanced Manufacturing Technology, Ranchi 834003, India, psmondalmbbox@gmail.com

* Correspondence: psmondalmbbox@gmail.com

Abstract: Low temperature dielectric property of charge/orbital ordered manganite, $\text{Pr}_{1-x}\text{Ca}_x\text{MnO}_3$ for $0.40 \leq x \leq 0.50$ is investigated systematically as a function of Ca-content, x . The Ca-content dependence of dielectric permittivity and dissipation factor exhibit distinct maxima around $x=0.45$. The overall dielectric response of charge ordered $\text{Pr}_{1-x}\text{Ca}_x\text{MnO}_3$ is dominated by polarization induced by polaron hopping and exhibits thermally activated relaxation behaviour. The dielectric relaxation behaviour over the investigated temperature range is analysed with the help of small polaron hopping model and as well as variable range hopping model. The estimated polaron parameters also display non-monotonic variation with x and exhibit broad minima between $x=0.425-0.45$. The observed results suggest that a modulation of checker board type charge ordering pattern in $\text{Pr}_{1-x}\text{Ca}_x\text{MnO}_3$ is possibly taking place in the Ca-content range of investigation $0.40 \leq x \leq 0.50$.

Keywords: Manganite, Charge/Orbital ordering, Dielectric property, Polaron

1. Introduction

Mixed valence perovskite manganite $\text{R}_{1-x}\text{A}_x\text{MnO}_3$ (R: trivalent rare earth and A: divalent alkaline earth) have renewed considerable interest after the discovery of colossal magnetoresistance [1-2]. The physical property $\text{R}_{1-x}\text{A}_x\text{MnO}_3$ involves complex interplay among charge, spin and orbital degree of freedoms [1]. It leads to appearance of wide variety of competitive phases with comparable energy scale across phase diagram, principally antiferromagnetic insulating (AFI) phase, ferromagnetic metallic (FMM) phase, ferromagnetic insulating (FMI) phase, paramagnetic insulating (PMI) phase and etc [1-3]. Often the competitive phase in manganite may co-exist over a range of length scales as a signature of electronic phase separation [4]. Of particular importance of present investigation is the charge/orbital ordered insulating (COI) phase in $\text{Pr}_{1-x}\text{Ca}_x\text{MnO}_3$ which appears along with CE-type of antiferromagnetic (AF) order in almost all perovskite type manganite near the half doping ($x=1/2$) where presence of equal amount of Mn^{3+} and Mn^{4+} is expected [5-6].

In general the COI phase appears in large bandwidth perovskite manganite only in a narrower doping range near $x=0.5$ [6]. However, for a narrow bandwidth manganite, like $\text{Pr}_{1-x}\text{Ca}_x\text{MnO}_3$, it is quite striking that the COI ground state exists over a

wider range i.e. $0.3 \leq x \leq 0.75$ [7-9]. The high temperature phase of $\text{Pr}_{1-x}\text{Ca}_x\text{MnO}_3$ is PMI where all the Mn-sites are appears to be equivalent. Below a critical temperature (e.g. $T_{\text{CO}} \sim 250\text{K}$ for $x=0.5$), the charge/orbital ordering transition is occurred concomitant with a structural transition where two distinct charge sites are stabilized by strong Coulomb interaction and also by the co-operative Jahn-Teller distortion of MnO_6 octahedra [9-12]. Further lowering the temperature the $\text{Pr}_{1-x}\text{Ca}_x\text{MnO}_3$ also exhibits a paramagnetic to antiferromagnetic transition (e.g. $T_{\text{N}} \sim 175\text{ K}$ for $x=0.5$) which is associated with an incommensurate to commensurate charge ordering transition [12].

It is well-known that the charge/orbital ordering phenomenon in $\text{Pr}_{1-x}\text{Ca}_x\text{MnO}_3$ is optimized at $x = 0.5$ where distinct Mn^{3+} and Mn^{4+} ions are spatially ordered in 1:1 ratio to form a perfect checkerboard-type (CB-type) charge/orbital ordering while a similar CB-type charge-ordered ground state for $0.30 < x < 0.50$ is also conceived to occur where the presence of extra Mn^{3+} ions is considered as structural defects [5, 11, 13-17]. However, this conventional site-centered CB-type of charge/orbital ordering picture has been highly debated and alternative pictures of charge/orbital ordering have been put forward [18-27]. Bond-centered ordering of Zener-polarons has been observed experimentally in $\text{Pr}_{1-x}\text{Ca}_x\text{MnO}_3$ near $x=0.40$ where the Mn-sites are remained equivalent and the charge is localized on bond [18]. The structural distortion associated with static long-range ordering of Zener-polarons results in noncentrosymmetric space group ($P2_1nm$) which interestingly allows for spontaneous electrical polarization [19, 20]. It has also been pointed out theoretically that the coexistence of CB-type of charge/orbital and Zener-polaron type (ZP-type) ordering can also be present in $\text{Pr}_{1-x}\text{Ca}_x\text{MnO}_3$ for intermediate compositions $0.40 < x < 0.50$. Interestingly, the coexistence of CB-type and ZP-type ordering can break the inversion symmetry and gives rise to ferroelectric instability [24]. Therefore, it is expected that the nature charge/orbital ordered phase in $\text{Pr}_{1-x}\text{Ca}_x\text{MnO}_3$ is not essentially same across the doping range $0.40 \leq x \leq 0.50$ instead, there is a possibility of evolution/modulation of charge ordering pattern. In spite of such expectations, no one reported clear evidence for such modulation of charge ordering pattern. However, in our earlier report we have shown abrupt change in physical properties in $\text{Pr}_{1-x}\text{Ca}_x\text{MnO}_3$ around $x \sim 0.425$, which can be interpreted as a phase transition between two different charge/orbital ordered phase [28].

Several experimental efforts have been devoted in order to investigate the role of charge ordering in intrinsic dielectric response in $\text{Pr}_{1-x}\text{Ca}_x\text{MnO}_3$ [29-33]. The $\text{Pr}_{1-x}\text{Ca}_x\text{MnO}_3$ are found to exhibit anomaly in dielectric constant at the vicinity of charge ordering transition temperature which suggests an important role of charge/orbital ordering in intrinsic dielectric response of $\text{Pr}_{1-x}\text{Ca}_x\text{MnO}_3$ [31, 33]. Lopes *et al.* observed a new phase transition in the temperature dependence of electric field gradient (EFG) measurements in $\text{Pr}_{1-x}\text{Ca}_x\text{MnO}_3$ which is also interpreted as an indirect evidence of local electric polarization due to charge/orbital ordering [34].

In the present article we have systematically studied the low temperature dielectric property of $\text{Pr}_{1-x}\text{Ca}_x\text{MnO}_3$ over the doping range $0.40 \leq x \leq 0.50$ with a close variation of Ca-content, x . We observe anomalous x -dependent behavior dielectric property in $\text{Pr}_{1-x}\text{Ca}_x\text{MnO}_3$ around Ca-content $x=0.45$. As a possible origin of the anomaly

in dielectric property the modulation/evolution of charge-ordered phase in $\text{Pr}_{1-x}\text{Ca}_x\text{MnO}_3$ for $0.40 \leq x \leq 0.50$ is endorsed.

2. Results

The systematic investigation of crystal structure of $\text{Pr}_{1-x}\text{Ca}_x\text{MnO}_3$ for $0.4 \leq x \leq 0.5$ has been done employing high resolution x-ray diffraction (HRXRD). All the compositions are single phased and at room temperature they exhibit orthorhombic unit cell with $Pnma$ space group. Estimated cell parameters, a , b and c and the cell volume V from the refinement of HRXRD data are found to be decreased monotonically as Ca-content, x gradually increases (Figure 1) which is in accordance with the smaller ionic radius of Ca^{2+} than that of Pr^{3+} .

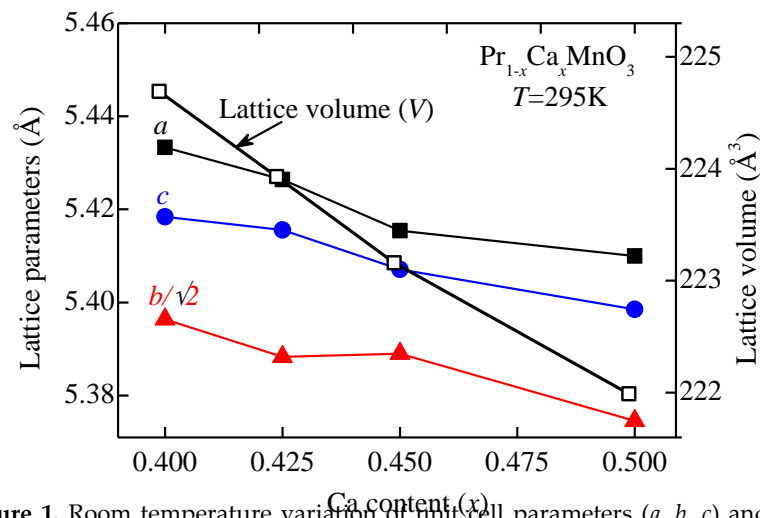


Figure 1. Room temperature variation of unit cell parameters (a , b , c) and unit cell volume, V of $\text{Pr}_{1-x}\text{Ca}_x\text{MnO}_3$ with orthorhombic ($Pnma$) setting as a function of Ca-content, x . Connecting lines guide to eye.

Real part of dielectric permittivity, $\epsilon'(\omega, T)$ versus temperature (T) patterns measured for several frequencies across the temperature range 4-150K for representative samples of $\text{Pr}_{1-x}\text{Ca}_x\text{MnO}_3$ with Ca-contents; $x=0.40$, 0.45 and 0.5 are shown in upper panels of figure 2. The dissipation factor $D(\omega, T)$ versus T plot for those compositions are also shown in the lower panels of figure 2. A typical feature of relaxation behaviour for all the samples can be observed. At temperature above 100K, $\epsilon'(\omega, T)$ reaching a value as high as $\epsilon' \sim 10^4$ with almost no variation with temperature and frequency and with decreasing temperature, $\epsilon'(\omega, T)$ shows step-like decrease and attains a nearly temperature and frequency independent value of about $\epsilon' \sim 30-50$. The characteristic temperature (T_F) at which the inflection in $\epsilon'(\omega, T)$ occurs is also associated with a peak in the corresponding $D(\omega, T)$ versus T plot which gradually shifts towards the higher temperature with increasing frequency. This confirms the thermally activated dielectric relaxation process [29, 30].

The isothermal dielectric permittivity $\epsilon'(\omega)$ and dissipation factor $D(\omega)$ as function of frequency are measured at $T = 4.5$ K and shown in upper and lower panels of figure 3(a), respectively. The

dielectric response in $\text{Pr}_{1-x}\text{Ca}_x\text{MnO}_3$ at higher temperature is usually dominated by the polarization induced by polaron hopping and exhibits thermally activated relaxation behaviour. However, at a

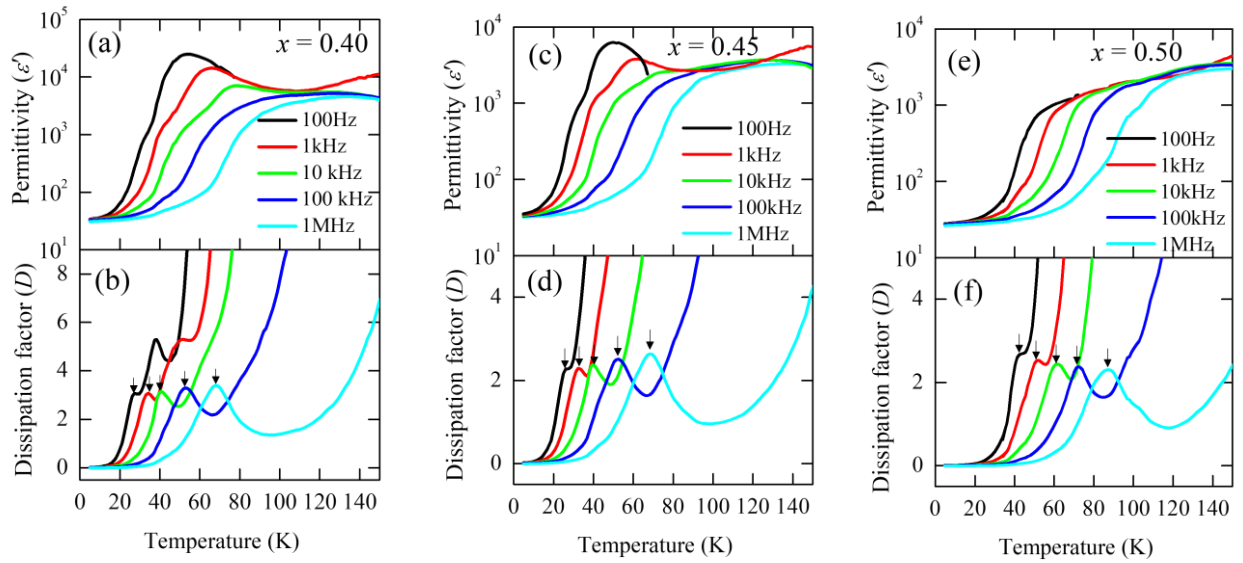


Figure 2. Dielectric properties of $\text{Pr}_{1-x}\text{Ca}_x\text{MnO}_3$ samples measured as function of temperature for test frequencies 100 Hz, 1 kHz, 10 kHz, 100 kHz and 1 MHz. The temperature variation of real part of dielectric permittivity (ϵ') for Ca-content (a) $x=0.40$, (c) $x=0.45$ and (e) $x=0.50$ (upper panels) and dissipation factor (D) for (b) $x=0.40$, (d) $x=0.45$ and (f) $x=0.50$ (lower panels). Arrows are indicating the peak positions.

sufficiently low temperature, the thermally activated charge carriers is frozen-out and the dielectric response is free from the relaxation behaviour due to polaron hopping and the dielectric response is dominated by the ionic-lattice contributions [35, 36]. As shown in figure 3(a), the frequency window (100Hz to 1MHz) over which the $\epsilon'(\omega)$ and $D(\omega)$ were measured is free from the typical dielectric relaxation due to polaron hopping and whatever frequency dispersion is observed at $T = 4.5$ K is arising from the ionic-lattice contributions. It is worthwhile to note that for the samples with $x=0.40$ and $x=0.50$, the $\epsilon'(\omega)$ and $D(\omega)$ show almost dispersion less behaviour whereas for $x=0.45$ exhibits significant frequency dispersion. In figure 3(b), we have plotted the variation of $\epsilon'(x)$ and $D(x)$ as functions Ca-content, x for 100 Hz and 1 kHz frequencies. For both the frequencies the $\epsilon'(\omega)$ and $D(\omega)$ exhibit similar x -dependence and one can observed conspicuous peak in $\epsilon'(x)$ and $D(x)$ at $x=0.45$.

The dielectric relaxation of $\text{Pr}_{1-x}\text{Ca}_x\text{MnO}_3$ is dominated by the polarization induced by thermally activated polaron hopping and as a signature; the shifting of peak position, T_P , towards the higher temperature with increasing relaxation frequency is clearly observed. We have analyzed the frequency dependence of T_P using small polaron hopping model (SPH) and also with Mott's variable-range-hopping (VRH) model. The relaxation frequency, f (or relaxation time, τ) of small polaron hopping is given by

$$fT_P = T_P\tau^{-1} = f_{01}\exp(-E_a/k_B T_P) \quad (1)$$

where E_a is the activation energy of the polaron hopping conduction, f_{01} is the pre-exponential factor and k_B is the Boltzmann's constant. In figure 4(a), the variation of $T_P\tau^{-1}$ is plotted as a function of $1000/T$ in the temperature range 25-90 K. The estimated values of E_a and f_{01} according to the SPH model are plotted as functions of x in upper and lower panels of figure 5(a), respectively. The value of the activation energy is in good agreement with that of charge-ordered manganite materials

reported earlier [29,30]. It can be seen that both the parameters E_a and f_{01} exhibit similar x -dependence. For $x = 0.40$ and 0.425 , the E_a -value slightly decreases from 44.7 meV to 38.6 meV with increase of x

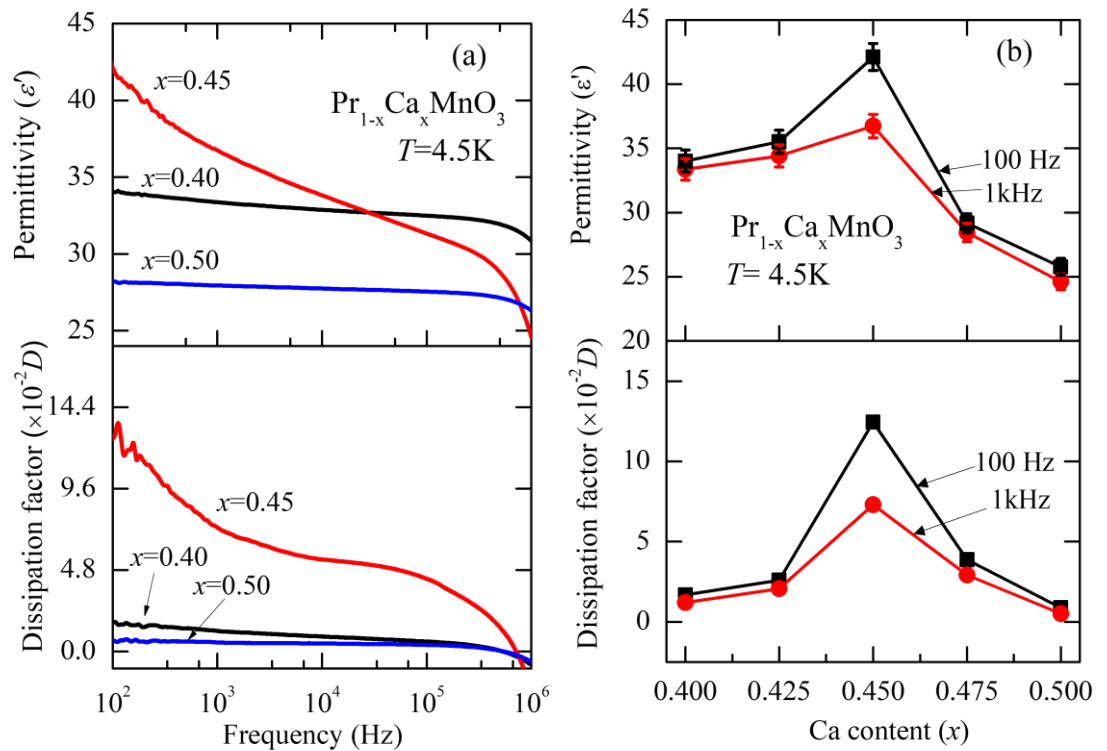


Fig.3. Dielectric properties of $\text{Pr}_{1-x}\text{Ca}_x\text{MnO}_3$ samples measured at 4.5 K. (a) Typical frequency dispersion pattern of real part of dielectric permittivity (upper panel) and dissipation factor (lower panel) for $\text{Pr}_{1-x}\text{Ca}_x\text{MnO}_3$ samples with different Ca-content, x . (b) The Ca-content, x variations of real part of dielectric permittivity (upper panel) and dissipation factor (lower panel) as a function of x . Connecting lines guide to eye.

while for $x = 0.45$ to 0.50 the E_a -value steadily increases from 40.3 meV to 79.6 meV with increase of x . In earlier publication we have reported similar x -dependence of the activation energy extracted temperature dependent resistivity data of $\text{Pr}_{1-x}\text{Ca}_x\text{MnO}_3$ for $0.40 \leq x \leq 0.50$ where the minimum E_a -value is also found near $x = 0.425$ [28]. This particular Ca concentration, $x = 0.425$ roughly corresponds to a phase boundary between two different charge/orbital ordered phases. It is worth mentioning that the E_a -values estimated from the dielectric relaxation are fairly similar to the activation energy for polaron hopping estimated from the resistivity data which also strongly indicate the polaronic nature of charge-ordered $\text{Pr}_{1-x}\text{Ca}_x\text{MnO}_3$.

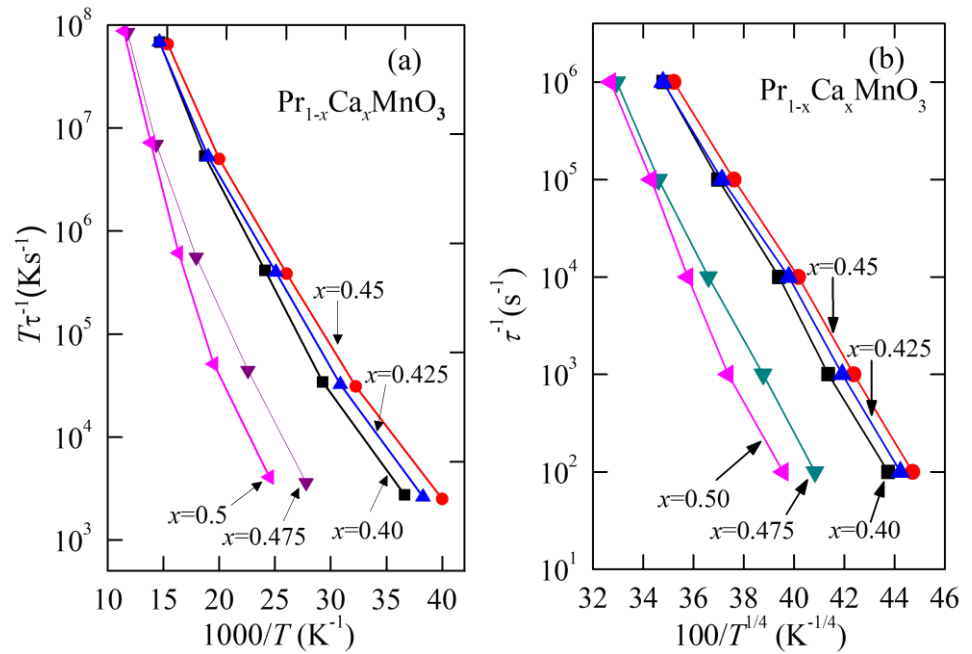
In the VRH, the relaxation frequency (or relaxation time τ) is given by

$$f = \tau^{-1} = f_{02} \exp \left(-(T_0/T_P)^{1/4} \right) \quad (2)$$

The f_{02} and T_0 are constant and T_0 is given by $T_0 = 24/\pi k_B N(E_F) \xi^3$, where $N(E_F)$ is the density of localized states at the Fermi level, and ξ is the decay length of the localized wave function. Figure 4(b) shows the variation of τ^{-1} as a function of $100/T$ in the temperature range 25-90 K. By comparing, the figure 4(a) and figure 4(b), it seems that the dielectric relaxation process can be explained well by VRH model rather than SPH model in the at least temperature range 25-90 K. The estimated values of T_0

and f_{02} from the VRH fitting are shown also in figure 5(b) as functions of x . Similar to SPH model both the parameters, T_0 and f_{02} also exhibit broad minima near $x=0.425$.

Figure 4. (a) The small polaron hopping (SPH) and (b) the variable range hopping (VRH)



plots of dielectric relaxations of $\text{Pr}_{1-x}\text{Ca}_x\text{MnO}_3$ samples with different Ca-content $x=0.40, 0.425, 0.45, 0.475$ and 0.50 . Connecting lines guide to eye.

In the VRH mechanism the hopping energy is given by $W = 0.25k_B T_0^{1/4} T^{3/4}$ and using the value of T_0 estimated from the fitting and taking $T = 50$ K, an average temperature around which the dielectric relaxation was measured, we obtain the values of polaron hopping energy, W of $\text{Pr}_{1-x}\text{Ca}_x\text{MnO}_3$ samples and plotted as a function of x in the upper panel of figure 5(a) alongside of $E_a(x)$ for comparison. The $W(x)$ is also shows similar Ca-content dependence like the activation energy, $E_a(x)$ estimated from SPH model.

3. Discussion

Let us turn our discussion towards the possible origin of observed anomalous x -dependence of dielectric properties. Presently, the origin observed peak in x -dependence of dielectric permittivity of $\text{Pr}_{1-x}\text{Ca}_x\text{MnO}_3$ near $x = 0.45$ is not clearly understood. However, two possible explanations can be drawn based on earlier literature: one possibility is related to inhomogeneous CB-type charge-ordered phase. The CB-type charge-orbital ordered phase in $\text{Pr}_{1-x}\text{Ca}_x\text{MnO}_3$ for $x \leq 0.50$ is susceptible to phase separation due to the presence of unequal amount of Mn^{3+} and Mn^{4+} ions. The evolution from homogeneous to inhomogeneous CB-type charge-ordered phase with decreasing x has found at a critical doping near $x=0.425$ [28, 34]. Therefore, the observed enhancement of dielectric constant near $x = 0.45$ may roughly corresponds to the phase boundary between inhomogeneous and homogeneous phases.

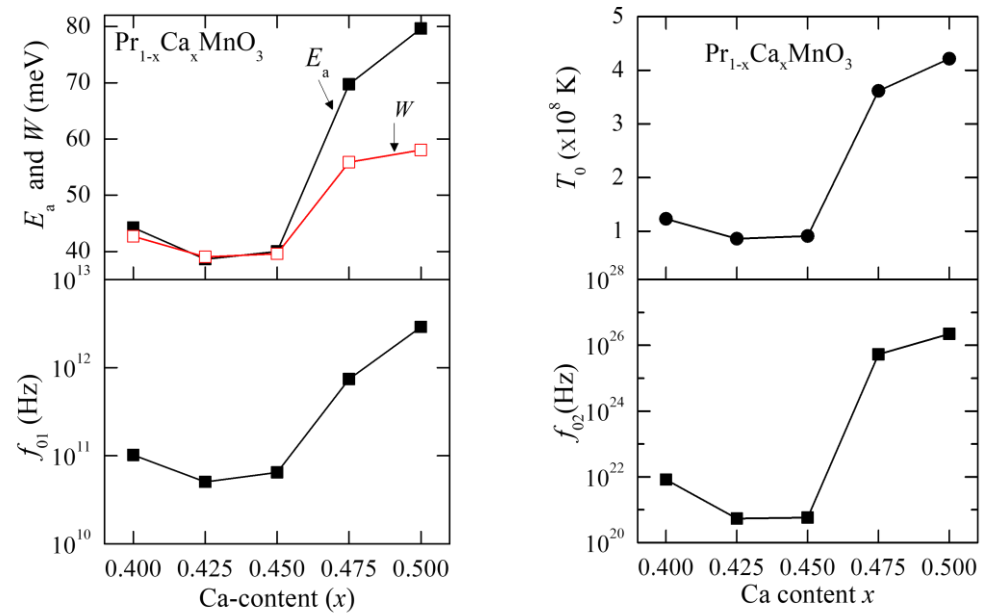


Figure 5. (a) Variation of activation energy, E_a (upper panel) and pre-exponential factor, f_{01} (lower panel) with x in $\text{Pr}_{1-x}\text{Ca}_x\text{MnO}_3$ samples, obtained from the fitting of $f(T)$ versus T data by small polaron hopping model. (b) Ca-content, x dependence of T_0 and pre-exponential factor, f_{02} estimated from variable range hopping model. The Ca-content x -dependence of the polaron hopping energy, W (open symbol), estimated from T_0 is also plotted in the upper panel of (a) along with the E_a . Connecting lines guide to eye.

Another possibility is based on formation of Zener-polaron-type ordered phase. In this context, the tight binding model calculation based on the degenerate double exchange framework have shown that the character of charge/orbital ordered phase in $\text{Pr}_{1-x}\text{Ca}_x\text{MnO}_3$ changes in a systematic manner from $x = 0.50$ down to 0.40.[24] The charge ordering pattern is found to be evolved from pure CB-type charge ordered phase at $x = 0.50$, to admixture phase of CB-type and ZP-type ordered phases with decreasing x and finally to a pure ZP-type ordered phase at $x = 0.40$. The admixture phase can break the inversion symmetry and leads to development of local ferroelectric moment. In fact the direct experimental evidence of subtle macroscopic ferroelectric polarization have recently been found in remnant electrical polarization measurement in $\text{Pr}_{1-x}\text{Ca}_x\text{MnO}_3$ samples [37,38] while indirect evidence of local ferroelectric moment have confirmed earlier in EFG measurement.[34]. Therefore, the observed peak in $\epsilon'(x)$ near $x = 0.45$ may probe a trace of the electronic ferroelectricity. However, direct measurement of the macroscopic electric polarization is difficult because of relatively high conductivity of $\text{Pr}_{1-x}\text{Ca}_x\text{MnO}_3$ samples (dissipation factor ~ 0.03) which can obscure the finite macroscopic polarization if there exists at least in the local scale. In addition, the charge ordered state in $\text{Pr}_{1-x}\text{Ca}_x\text{MnO}_3$ can be collapsed by sufficient electric field and gives huge electroresistance effect which further complicates experimental situation to directly probe the macroscopic polarization [39]. Furthermore, the $\text{Pr}_{1-x}\text{Ca}_x\text{MnO}_3$ sample with $x=0.45$ exhibits stronger frequency dispersion in $\epsilon'(\omega)$ and $D(\omega)$ than the two end compositions and consequently it indicates stronger tendency towards the phase separation[40]. Therefore the observed result strongly suggests the presence of an admixture phase in the intermediate composition range which possibly comprised of ZP-type and CB-type ordered phases.

4. Materials and Methods

For this study polycrystalline samples with nominal compositions of $\text{Pr}_{1-x}\text{Ca}_x\text{MnO}_3$ ($x=0.40, 0.425, 0.450, 0.475$ and 0.50) were synthesized by a conventional solid state reaction method. The stoichiometric mixtures of the starting materials, Pr_2O_3 (3N), CaCO_3 (3N) and MnO_2 (3N) were calcined at 1373K in air for 24 hours. The calcined powders were pressed into circular pellets form and sintered at 1673 K in air for 48 hours. The detailed structural characterizations and physical property measurements were carried out on the as-synthesized samples which were reported in our earlier publication [28]. The temperature dependent dielectric property was measured in the frequency range 100Hz to 1MHz by using LCR meter (Agilent) from 4 to 150 K. The circular disc-shaped samples with typical diameter ~8 mm and thickness ~0.5 mm were used for the measurement. For electrode, air-drying silver pasted was coated on pellet surfaces and cured at 623K.

5. Conclusions

In summary, the low temperature dielectric property of charge ordered manganite $\text{Pr}_{1-x}\text{Ca}_x\text{MnO}_3$ for $0.40 \leq x \leq 0.50$ is investigated systematically as a function of Ca-content, x . The Ca-content dependence of dielectric permittivity exhibits distinct maxima around $x=0.45$. The overall dielectric response exhibits thermally activated relaxation behaviour. The estimated polaron parameters i.e. the activation energy of polaron hopping and polaron hopping frequency also show broad minima between $x=0.425$ and 0.45 . The observed results suggest that the modulation of checkerboard type charge ordering pattern in $\text{Pr}_{1-x}\text{Ca}_x\text{MnO}_3$ is possibly taking place which further supports the conjecture of having phase boundary between different charge-orbital ordered phases near $x=0.425$ reported in our earlier publication. If we consider the Zener-polaron phase and the checkerboard type charge ordered phase below and above the boundary, we ascribe the noticeable enhancement of the dielectric permittivity to the instability to the electronic ferroelectricity.

Author Contributions: Supervision, Conceptualization, Reviewing and Editing, Partha Sarathi Mondal; Methodology, Validation, Partha Sarathi Mondal and Ankit Kumar Singh; Formal Analysis, Original draft preparation, Visualization Ankit Kumar Singh.

Funding: Please add: This research was partially funded by DST-SERB, Government of India (grant no. CRG/2019/00006618).

Data Availability Statement: Not applicable”.

Acknowledgments: Authors also gratefully acknowledge I. Terasaki and R. Okazaki for valuable discussions.

Conflicts of Interest: The authors declare no conflict of interest.

References

1. T. Tokura, *Colossal Magnetoresistive Oxides* (Gordon and Breach Science, Amsterdam, 2000).
2. J. van den Brink, G. Khaliullin, and D. I. Khomskii, *Colossal Magnetoresistive Manganites* ed. T. Chatterji (Kluwer, Dordrecht, 2002).
3. E. Dagotto, *Nanoscale Phase Separation and Colossal Magnetoresistance, Springer Series in Solid-State Sciences* (Springer, New York, 2003).
4. M. Uehara, S. Mori, C. H. Chen, and S. W. Cheong, *Nature* (London) 399(1999)560.
5. J. B. Goodenough, *Phys. Rev.* 100 (1955)564.
6. C. N. R. Rao, A. Arulraj, P. N. Santosh, and A. K. Cheetham, *Chem. Mater.* 10(1998)2714.
7. E. Pollert, S. Krupicka, and E. Kuzmicova, *J. Phys. Chem. Solids* 43(1982)1137.
8. Z. Jirak, S. Krupicka, Z. Simsa, M. Dloua, and S. Vratilav, *J. Magn. Magn. Mater.* 53(1985)153.

9. P. G. Radaelli, D. E. Cox, M. Marezio and S. W. Cheong, Phys. Rev. B 55(1997)3015.
10. D. I. Khomski, *Spin Electronics*, ed. M. Ziese and M. J. Thornton (Springer, Berlin, 2001)
11. Y. Tomioka, A. Asamitsu, H. Kuwahara, Y. Moritomo, and Y. Tokura, Phys. Rev. B 53 (1996)R1689.
12. C. H. Chen, S. Mori, and S. W. Cheong, Phys. Rev. Lett. 83(1999)4792.
13. T. Asaka, S. Yamada, S. Tsutsumi, C. Tsuruta, K. Kimoto, T. Arima, and Y. Matsui, Phys. Rev. Lett. 88(2002)097201.
14. S. Mori, T. Katsufuji, N. Yamamoto, C. H. Chen, and S.W. Cheong, Phys. Rev. B 59(1999)13573.
15. R. Kajimoto, H. Yoshizawa, Y. Tomioka, and Y. Tokura, Phys. Rev. B 63(2001)212407.
16. M. V. Zimmermann, C. S. Nelson, J. P. Hill, D. Gibbs, M. Blume, D. Casa, B. Keimer, Y. Murakami, C. C. Kao, C. Venkataraman, T. Gog, Y. Tomioka, and Y. Tokura, Phys. Rev. B 64 (2001)195133.
17. A. Yakubovskii, A. Trokiner, S. Verkhovskii, A. Gerashenko, and D. I. Khomskii, Phys. Rev. B 67(2003)064414.
18. A. Daoud-Aladine, J. Rodriguez-Carvajal, L. Pinsard-Gaudart, M. T. Fernandez-Diaz, and A. Revcolevschi, Phys. Rev. Lett. 89(2002)097205.
19. L. Wu, R. F. Klie, Y. Zh and Ch. Joos, Phys. Rev. B 76(2007)174210.
20. Ch. Joos, L. Wu, T. Beetz, R. F. Klie, M. Beleggia, M. A. Schofield, S. Schramm, J. Hoffmann, and Y. Zhu, Natl. Acad. Sci. (USA) 104 (2007)13597.
21. S. Grenier, J. P. Hill, D. Gibbs, K. J. Thomas, M. v. Zimmermann, C. S. Nelson, V. Kiryukhin, Y. Tokura, Y. Tomioka, D. Casa, T. Gog, and C. Venkataraman, Phys. Rev. B 69 (2004)134419.
22. K. J. Thomas, J. P. Hill, S. Grenier, Y -J Kim, P. Abbamonte, L. Venema, A. Rusydi, Y. Tomioka, Y. Tokura, D. F. McMorrow, G. Sawatzky, and M. van Veenendaal, Phys. Rev. Lett. 92(2004)237204.
23. R. J. Goff and J. P. Attfield, Phys. Rev. B 70(2004)140404(R).
24. D. V. Efremov, J. van den Brink, and D. I. Khomskii, Nat. Mater. 3(2004)853.
25. G. Giovannetti, S. Kumar, J. van den Brink, and S. Picozzi, Phys. Rev. Lett. 103(2009)037601.
26. G. Colizzi, A. Filippetti, and V. Fiorentini, Phys. Rev. B 82(2010)140101(R).
27. K. Yamuchi and S. Picozzi, J. Phys. Soc. Jpn. 82(2013)113703.
28. P. S. Mondal, S. Asai, T. Igarashi, T. Suzuki, R. Okazaki, I. Terasaki, Y. Yasui, K. Kobayashi, R. Kumai, H. Nakao, and Y. Murakami, J. Phys. Soc. Jpn. 83 (2014)064709.
29. Y. Yamada, T. Arima and K. J. Takita, Phys. Soc. Japan 68 (1999)3701.
30. C. C. Wang and L. W. Zhang, New J. Phys. 9 (2004)210.
31. S. Mercone, A. Wahl, A. Pautrat, M. Pollet, and C. Simon, Phys. Rev. B 69(2004)174433.
32. R. S. Freitas, J. F. Mitchel, and P. Schiffer, Phys. Rev. B 72(2005)144429.
33. N. Biskup, A. de Andres and J. L. Martinez, Phys. Rev. B 72(2005)024115.
34. A. M. L. Lopes, J. P. Araujo, V. S. Amaral, J. G. Correia, Y. Tomioka, and Y. Tokura Phys. Rev. Lett. 100(2008)155702.
35. J. L. Cohn, M. Peterca, and J. J. Neumeier, Phys. Rev. B 70(2004)214433.
36. K. P. Neupane, J. L. Cohn, H. Terashita, and J. J. Neumeier, Phys. Rev. B 74(2006)144428.
37. V. K. Shukla, S. Mukhopadhyaya, K. Das, A. Sharma and I. Das, Phys. Rev. B 90 (2014)245126.
38. V. K. Shukla and S. Mukhopadhyaya, RSC Adv. 6(2016)93130.
39. A. Asamitsu, Y. Tomioka, H. Kuwahara, and Y. Tokura, Nature 388(1997)50.
40. Z. Sheng, M. Nakamura, F. Kagawa, M. Kawasaki and Y. Tokura, Nat. Commun. 3(2012)944.